Real-time x-ray studies of gallium adsorption and desorption

Ahmet S. Özcan, Yiyi Wang, Gozde Ozaydin, Karl F. Ludwig, Anirban Bhattacharyya, Theodore D. Moustakas, and D. Peter Siddons

Citation: Journal of Applied Physics **100**, 084307 (2006); doi: 10.1063/1.2358307
View online: http://dx.doi.org/10.1063/1.2358307
View Table of Contents: http://scitation.aip.org/content/aip/journal/jap/100/8?ver=pdfcov
Published by the AIP Publishing

Real-time x-ray studies of gallium adsorption and desorption

Ahmet S. Özcan,[a] Yiyi Wang, Gozde Ozaydin,[b] and Karl F. Ludwig
Physics Department, Boston University, Boston, Massachusetts 02215

Anirban Bhattacharyya and Theodore D. Moustakas
Department of Electrical and Computer Engineering, Boston University, Boston, Massachusetts 02215

D. Peter Siddons
National Synchrotron Light Source, Brookhaven National Laboratory Upton, New York 11973

(Received 14 April 2006; accepted 24 July 2006; published online 18 October 2006)

Real-time grazing-incidence small-angle x-ray scattering has been employed to study the adsorption and desorption of Ga on *c*-plane sapphire and Ga-polar GaN surfaces. Formation of self-organized liquid Ga nanodroplets has been observed on sapphire during Ga exposure from an effusion cell at high flux. Subsequent to the Ga deposition, the nanodroplets were nitridated *in situ* by a nitrogen plasma source, which converted the droplets into GaN nanodots. In addition to the droplet studies, at lower Ga flux, the adsorption and desorption of Ga have been studied in the predroplet regime. For identical processing conditions, significantly different Ga adsorption/desorption rates were observed on sapphire and GaN surfaces. © *2006 American Institute of Physics*.
[DOI: 10.1063/1.2358307]

I. INTRODUCTION

Wide-band gap III-V nitrides, such as GaN and its alloys, have important applications in optoelectronics and high-power devices. One of the commonly employed methods for growing GaN thin films is molecular beam epitaxy (MBE). The MBE technique utilizes effusion cells as metal sources and a reactive gas or a plasma source as the nitrogen source. Because of the lack of lattice matched substrates, GaN thin films are most commonly grown on sapphire, which has a good crystalline quality and relatively low cost.

One of the most important growth parameters that control the properties of GaN films is the metal/nitrogen atomic flux ratio.[1–3] GaN deposition is typically performed under metal-rich conditions, which produces better quality and smoother films. Previous studies[1–4] have shown that during Ga-rich growth, under certain conditions, a liquid Ga adlayer forms on the surface. It has been suggested that the Ga adlayer acts as an autosurfactant and enhances the migration of N atoms on the surface. However, very high Ga/N atomic flux ratios and/or low substrate temperatures during growth typically cause macroscopic Ga droplet formation on the surface due to excess Ga, which is detrimental for device applications. Hence, there is an optimum process window, which is a detailed balance of atomic fluxes and the substrate temperature that produces good quality films in terms of morphological, optical, and electronic properties. The equilibrium thickness of the liquid Ga adlayer and its structure during Ga-rich growth has not been well understood and is still an active research area.

Because of the technological motivations for growing good quality GaN films, studies of Ga adsorption and desorption have been carried out on different surfaces using reflection high-energy electron diffraction (RHEED) and mass spectroscopy.[5–9] Although these techniques provide important information on the rates of Ga adsorption and desorption, they do not monitor the evolution of the surface morphology. Here we report real-time surface x-ray studies of Ga adsorption/desorption on sapphire and GaN at high temperatures. These monitored the surface morphology evolution as well as the adsorption/desorption kinetics.

II. EXPERIMENTAL DETAILS

Gallium adsorption and desorption studies utilized synchrotron-based grazing-incidence small-angle x-ray scattering (GISAXS). The GISAXS technique[10] is sensitive to nanometer-size morphological changes on the surface, such as roughening and island formations. Typically, GISAXS measurements can monitor lateral length scales between 5 and 150 nm at the surface. The GISAXS geometry used in our experiments is shown in Fig. 1.

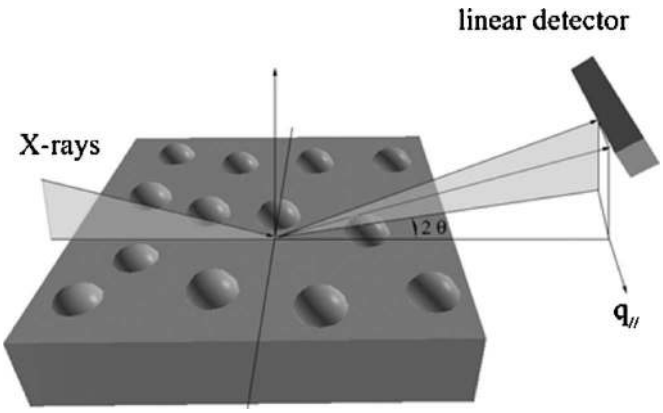

FIG. 1. The scattering geometry of the GISAXS. The linear detector is placed parallel to the sample surface to measure the scattering as a function of $q_{\parallel}$.

[a]Also at IBM Microelectronics, Fishkill, NY.
[b]Also at the Aerospace and Mechanical Engineering Department.

The experiments were performed in an ultrahigh vacuum (UHV) x-ray diffraction chamber with a base pressure of 10^{-9} Torr. A dual filament Applied Epi SUMO effusion cell was employed for Ga deposition. The real-time x-ray experiments were performed on the beamline X21 of the National Synchrotron Light Source at Brookhaven National Laboratory.[11] The GISAXS intensity was collected by a one-dimensional (1D) position sensitive detector (PSD) with 1 s time resolution. For the real-time GISAXS scans, the incidence angle was kept constant at 1°, while the exit angle was near the critical angle (0.2°) to the sample surface to enhance surface sensitivity. This geometry gives $q_z=1$ nm^{-1} (momentum transfer perpendicular to the surface). The asymmetric scattering geometry is chosen to avoid going directly through the specular rod itself—instead the GISAXS passes through the tail of the specular rod and $q_{\|}$, the momentum transfer parallel to the surface can be small (0.005 nm^{-1}), but is never zero. We will refer to the GISAXS peak near $q_{\|}=0$ as the "near-specular" peak. Gallium adsorption/desorption studies were performed on *c*-plane sapphire and on Ga-polar GaN samples. The sapphire samples were small cuts from "epitaxial" quality commercial wafers. The GaN sample was grown by plasma-assisted MBE using a three-step method. First, the substrate, which is a *c*-plane sapphire wafer, was nitridated by exposure to nitrogen plasma at 870 °C. An AlN buffer layer was then deposited at the same temperature, followed by growth of (0001) GaN at temperatures of 750–800 °C. The thickness of the GaN film was approximately 0.7 μm.

During Ga adsorption/desorption studies the sample temperature was monitored by a pyrometer and a thermocouple at the back of the sample heater. Prior to the Ga adsorption experiments, the samples were degassed by annealing in UHV at 800 °C for at least 30 mins. RHEED analysis was performed to confirm the orientation and the smoothness of the starting surface.

III. RESULTS

A. Ga adsorption/desorption on sapphire in the droplet regime

Figure 2 shows the GISAXS time evolution of the sapphire sample during Ga adsorption at 700 °C. The scattering intensity was collected by a (1D) PSD with 1 s time resolution. The Ga cell temperature was 1040 °C, which corresponds to an equilibrium vapor pressure of 8×10^{-3} Torr above the Ga in the cell. There has been uncertainty in the literature on the temperature dependence of the condensation pressure of Ga.[12,13] According to the equation presented by Alcock *et al.*,[13] the equilibrium vapor pressure of Ga at a sample temperature of 700 °C is 1.75×10^{-6} Torr. Our measurements show that the beam equivalent pressure (BEP) on the sample was in the low 10^{-6} Torr range, which is in close vicinity to the condensation pressure at this sample temperature. A remotely controlled shutter in front of the effusion cell adjusted the timing of the Ga beam exposure. The total exposure of Ga was 10 s for the scan shown in Fig. 2. Initially, the scattering profile shows only the intensity of the near-specular reflection from the sample surface. At approximately $t=15$ s, the Ga shutter was opened and, as Ga exposure continues, the broad diffuse scattering background evolves into symmetric peaks centered on approximately $|q_{\|}|=0.12$ nm^{-1}. These peaks indicate the formation of laterally correlated Ga droplets with an average real-space distance of approximately 50 nm.

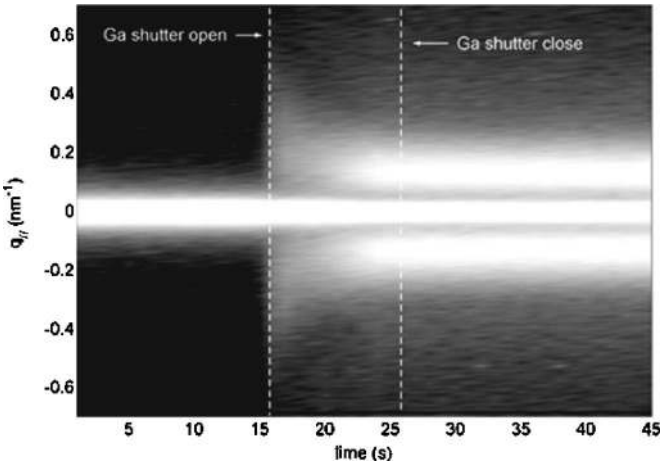

FIG. 2. The real-time GISAXS evolution of the sapphire surface during Ga adsorption and desorption at 700 °C. The scan was taken at $q_z=1$ nm^{-1}.

After the real-time GISAXS scan shown in Fig. 2 was terminated, the 1-*d* detector was scanned continuously along q_z from 0.5 to 2 nm^{-1} during desorption in order to monitor the height evolution of the droplets. The Ga source was shuttered during these scans. It took 1 min to complete and start each subsequent q_z scan. The Ga desorption at this substrate temperature was sufficiently slow that the evolution during each scan was negligible. Figure 3 shows the snapshots of the GISAXS scan during desorption. These scans show that the original GISAXS q_z map of the bare sapphire was recovered after approximately 65 min, which suggests the complete desorption of Ga from the surface. The RHEED analysis immediately after the real-time x-ray measurements also

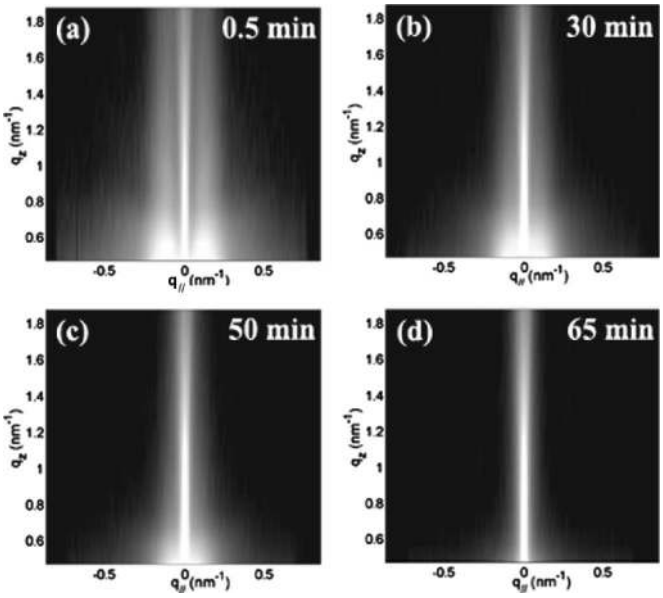

FIG. 3. Selected GISAXS q_z scans during desorption after 10 s Ga exposure.

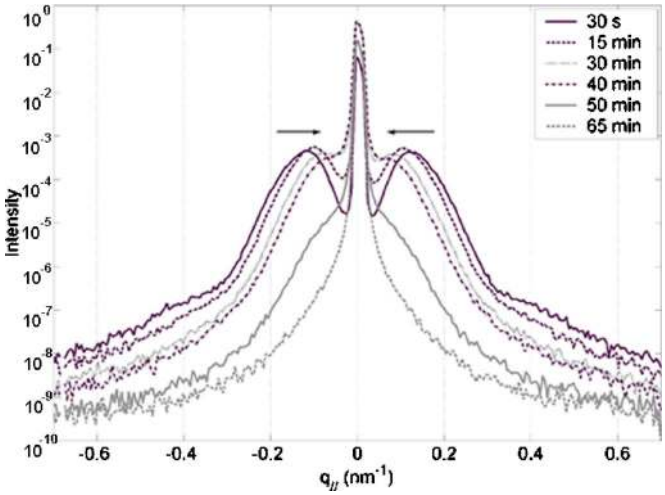

FIG. 4. Selected slices from the real-time GISAXS q_z scans at q_z $=0.5$ nm^{-1}, which shows the evolution of the surface morphology during desorption.

confirmed the originally observed streaky sapphire surface pattern. Figure 4 shows slices of selected q_z scans taken at $q_z=0.5$ nm^{-1} during desorption.

In order to estimate the height of the Ga droplets, the q_z dependence of the GISAXS measurements was analyzed using the Guinier approximation.[14] According to the Guinier approximation the scattered intensity is related to the wave vector q as

$$I(q) \sim \exp(-R^2q^2), \tag{1}$$

where R is the radius of gyration, which gives approximately the cluster size. Therefore, from the slope of the plot of $\log(I)$ vs q_z^2 the height of the droplets can be estimated. The Guinier plot obtained from the GISAXS measurement shown in Fig. 3(a) is drawn in Fig. 5. The linear decrease at very low q_z values, which does not evolve in time, results from dynamical scattering from the substrate and the film. The average droplet height was calculated using the slope obtained from the linear fit result shown in Fig. 5. Using the relation of Eq. (1) and the slope from the fit, the droplets are calculated to be approximately 3.3 nm high.

The lateral correlation length obtained from GISAXS analysis indicates the average distance between Ga droplets.

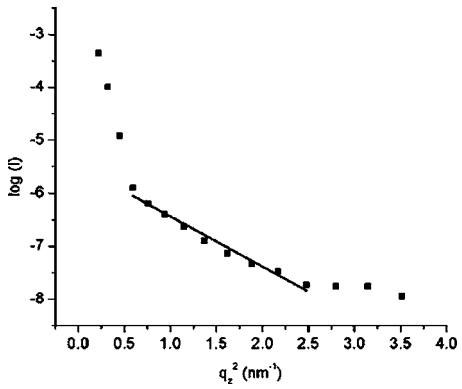

FIG. 5. The Guinier plot obtained from the GISAXS measurement taken 30 s after the Ga deposition has terminated. The solid line indicates the linear fit to the data.

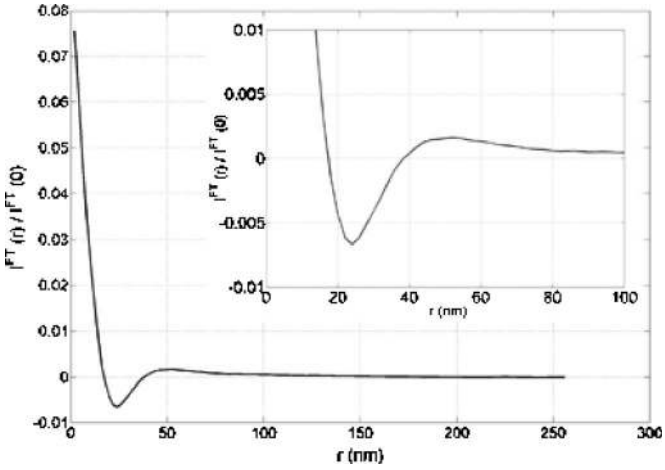

FIG. 6. Fourier transform of the measured GISAXS at $q_z=0.5$ nm^{-1}, which gives approximately the real-space electron density correlation. The peak at 50 nm indicates the average spacing between droplets and the intensity decay at smaller r values corresponds to the electron density distribution of individual droplets.

Quantitative analysis of the GISAXS scans shows that the correlation size of the Ga droplets increases during desorption, which is observed by the inward shift of the side peaks in Fig. 3. The slices obtained from q_z scans (Fig. 4) show that, after the Ga shutter was closed, the average distance between droplets increased from approximately 50 to 100 nm.

In order to get information on the mean droplet lateral size, one can use an approach known from small-angle scattering theory. The analysis is based on obtaining the real-space correlation function of the electron density by taking the Fourier transform of the GISAXS profile. The details of this analysis can be found in Ref. 15. Figure 6 shows the Fourier transform of the measured GISAXS profile shown in Fig. 3(a), at $q_z=0.5$nm^{-1}. The central peak close to $r=0$ corresponds to the mean electron density distribution of individual droplets. Twice the half-width at half maximum (HWHM) of this peak gives an approximate value for the droplet size, which is roughly 16 nm in this case. The peak in Fig. 6 at $r=50$ nm corresponds to the average distance between the dots, in agreement with the analysis of the measured GISAXS profiles.

B. Plasma nitridation of Ga nanodroplets

In order to study the droplets in real space, some of the samples were exposed to nitrogen plasma, which froze the motion of Ga adatoms and solidified the Ga droplets. The active nitrogen species coming from the plasma source reacted with the Ga droplets on the surface and transformed them into GaN nanodots. The detailed results of these experiments are discussed elsewhere.[16] Our real-time GISAXS measurements during the process showed that the surface morphology evolution is arrested once the liquid droplets are exposed to the nitrogen plasma. Therefore, the *ex situ* atomic force microscope (AFM) analysis of the GaN nanodots can provide information on the size and distribution of the Ga nanodroplets. The AFM analysis of a sapphire sample with the GaN nanodots is seen in Fig. 7. The section analysis of

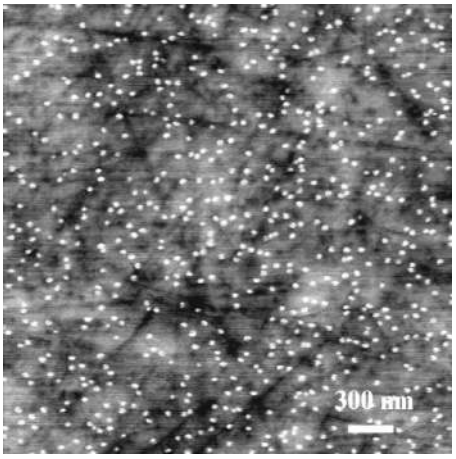

FIG. 7. The AFM analysis of the Ga nanodots on sapphire, showing a 3 $\times 3$ μm^2 AFM topograph.

the AFM micrographs shows that the average GaN dot diameter is approximately 30 ± 15 nm and the typical height of the dots is 2–3 nm. Because of the tip convolution effects, the sizes measured by AFM can be taken as an upper limit.

C. Ga adsorption/desorption on sapphire in the predroplet regime

In order to study the adsorption/desorption process in the predroplet regime, some of the studies have been performed at lower Ga fluxes. In the predroplet regime, desorption is much faster than is the case once droplets form. For these measurements, the Ga cell temperature was 933 °C, which corresponds to an equilibrium vapor pressure in the Ga cell of approximately 1×10^{-3} Torr. According to our measurements, the BEP on the sample is below the condensation pressure at this sample temperature. In this regime, real-time GISAXS scans did not develop any correlation peaks during Ga deposition. Moreover, *in situ* reflectivity scans did not show oscillations suggesting that the Ga did not form a smooth layer on the surface. However, the near-specular ($q_{\|}=0$) part of the GISAXS spectrum was very sensitive to the roughness changes induced by Ga adsorption. Figure 8(a) shows the real-time intensity evolution of the near-specular peak for different Ga adsorption periods at constant flux. The near-specular peak intensity decreased as soon as Ga adsorption commences, showing that roughness increased and the substrate reflectivity decreased due to the arrival of adatoms on the surface. The intensity of the diffuse scattering from

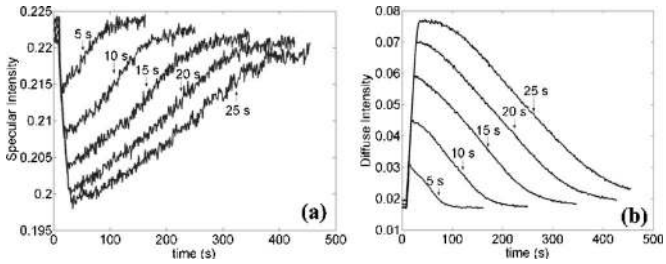

FIG. 8. The intensity evolution of the (a) near-specular and (b) diffuse parts of the GISAXS profiles in the predroplet regime as a function of Ga exposure time. The sapphire substrate temperature was 700 °C.

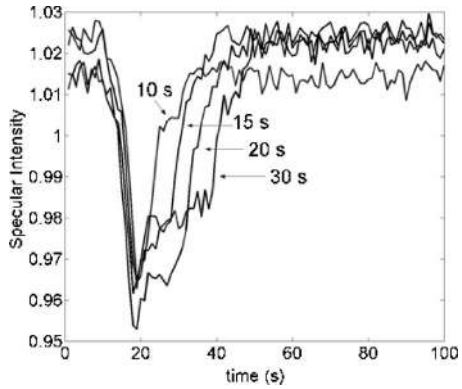

FIG. 9. The intensity evolution of the near-specular part of the GISAXS profile during Ga adsorption/desorption on GaN at 700 °C.

surface roughness, i.e., the nonspecular part of GISAXS increased. The time evolution of the diffuse scattering during Ga adsorption, which is obtained by integrating the total GISAXS intensity except the near-specular peak, is plotted in Fig. 8(b). These results show that, with increasing Ga exposure, further roughening occurs, which suggests continuous accumulation of adatoms. However, the x-ray intensity should not be taken as a direct measure of the number of Ga adatoms.

D. Ga adsorption/desorption on GaN in the predroplet regime

The adsorption and desorption of Ga were also studied on a Ga-polar GaN sample, which was grown on *c*-plane sapphire. In order to compare the results to those obtained for the sapphire surface (shown in Fig. 8), the Ga flux and the sample temperature were kept the same. Figure 9 shows the time-resolved intensity evolution of the near-specular part of the GISAXS spectrum during Ga adsorption and desorption. Similar to the case for the sapphire surface, at this Ga flux and sample temperature no droplet formation occurred. However, in contrast to the results for the sapphire surface, Ga exposure for more than 10 s did not cause further changes in the x-ray scattering profile. In other words, at this sample temperature and Ga flux, the adsorption and desorption reached equilibrium in approximately 10 s, which indicates a faster desorption rate compared to the sapphire. According to the x-ray results, the rate of Ga desorption from GaN is approximately six times faster than the rate of desorption from the sapphire surface. This result is inconsistent with the reported Ga desorption activation energies of 2.2 eV from Ga-polar GaN and 2.05 eV from *c*-plane sapphire.[9] However, the discrepancy may simply be due to the different prefactors in the thermally activated desorption kinetics.

IV. DISCUSSION

Previous studies of Ga adsorption and desorption on SiC concluded that Ga adsorption proceeds in the Stranski-Krastanow (SK) mode.[5] In the SK mode, first a wetting layer covers the substrate, and after a critical thickness is reached, growth continues in three-dimensional (3D) mode driven by strain, where droplets or islands form. Studies[5,7] which uti-

lized real-time RHEED have observed an oscillation of the specular reflection that could be interpreted as the formation of a wetting layer. It is common to observe droplet formation for liquids on surfaces. This phenomenon does not require strain mismatch but occurs due to high surface tension. Therefore we base our discussion below on interface and surface tension driven droplet formation rather than the strain-driven SK growth.

In order to better understand the adsorption and desorption of Ga on sapphire and GaN the surface atomic structures have to be considered. Atomically smooth *c*-plane sapphire (Al_2O_3) surface may have Al or O terminations. Detailed crystal truncation rod experiments[17] have shown that unreconstructed Al_2O_3 substrates that were annealed in air at temperatures higher than 1200 °C have smooth surfaces and that they are terminated by a single layer of Al. Although RHEED analysis of our samples shows streaky patterns, our samples did not go through the high temperature air annealing treatment. Therefore we expect that the sapphire surface prior to Ga adsorption may have a mixture of Al and O terminating layers. At high temperatures, Ga atoms adsorbing on the surface may form bonds to the O atoms. It is assumed that the adsorbed metal atom loses charge to the surface oxygen(s) to form bonds, which could be as strong as the Al–O bonds in the bulk.[18]

The interaction of a liquid Ga adlayer on GaN would be quite different. Wurtzite GaN can exist in two inequivalent surface orientations, denoted as Ga polar and N polar. The sample used in this study was grown as Ga polar. According to theoretical calculations for possible Ga adlayer structures,[4] N-polar surface stabilizes a single monolayer of Ga, bonded to the top GaN bilayer. On the other hand, Ga-polar surface would stabilize a laterally contracted Ga bilayer. Under Ga-saturated conditions the Ga atoms will be held by weak, delocalized Ga–Ga metallic bonds. Therefore, as observed in our data, Ga desorption would be easier from the GaN surface than from Al_2O_3, which could stabilize a Ga adlayer due to stronger Ga–O bonds.

At the substrate temperature used in this study (700 °C) Ga forms a liquid adlayer on the surface. Hence, liquid droplet formation due to surface tension is not surprising. Self-organized droplet formation has been previously observed in "droplet epitaxy" studies of group III-arsenides.[19,20] The droplet epitaxy method starts with the adsorption of the group-III metal, such as Ga or In, and subsequent crystallization by As exposure and annealing. So far no detailed understanding of the lateral droplet correlations has been proposed in these studies.

According to theoretical models,[21–23] the evolution of droplet formation typically involves nucleation, coalescence, and ripening processes. The droplets may nucleate heterogeneously at specific sites such as on impurities or imperfections on the surface or nucleate homogeneously. Simulations[23] of homogeneous nucleation of droplets have shown the coexistence of monodispersed large droplets with polydispersed small droplets that form due to continuous nucleation. However, in the simulations, simultaneous heterogeneous nucleation results only in a monodisperse distribution of droplets. The development of a peak in the GISAXS pattern and the *post facto* AFM measurements on the GaN dots suggests the presence of a relatively monodisperse distribution of droplets.

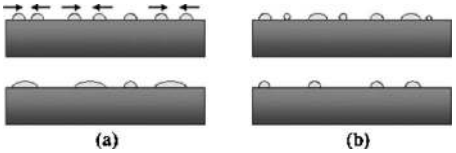

FIG. 10. Illustrations of possible Ga desorption models: (a) coalescence and (b) inhomogeneous desorption.

According to the x-ray and AFM analysis, the Ga droplets have small aspect ratios. The average height and the lateral sizes of the droplets, which are 3 and 30 nm, respectively, suggest that the approximate wetting angle is 140°. The large wetting angle indicates that Ga almost wets the sapphire surface.

Another phenomenon observed by our real-time results is the coarsening of the correlation size during desorption. This could be understood by at least two possible scenarios. The simplest explanation valid for any liquid droplet system, as long as there is sufficient energy for surface migration, is droplet coalescence. In this case, the real-time data suggest that during desorption, Ga droplets coalesce due to high surface mobility induced by high temperature and finally evaporate from the surface. In a second possible scenario, due to size differences, Ga droplets may desorb inhomogenously. Smaller droplets will diminish and desorb earlier, which will increase the average distance between droplets in time. These two models are depicted in Fig. 10.

V. CONCLUSIONS

In conclusion, we have demonstrated that real-time GISAXS can be used as an in situ technique to study adsorption and desorption of Ga at high temperatures and in an UHV environment. At high Ga atomic flux, we have observed the formation of nanoscale Ga droplets on sapphire that are laterally correlated. For lower Ga flux, adsorption and desorption were studied as a function of Ga exposure time. Under identical experimental conditions, the Ga adatoms continue to accumulate on sapphire as long as Ga is supplied; however on a GaN surface the Ga adatoms reach an equilibrium adlayer thickness. This suggests that Ga adatoms are more strongly bonded to the sapphire surface than to the GaN surface. Further studies will focus on the kinetics of Ga adsorption/desorption on various surfaces using real-time x-ray scattering.

ACKNOWLEDGMENTS

This work was partially supported by DOE DE-FG02-03ER46037 and NSF DMR-0507351. The real-time x-ray system for surface processes was made possible by NSF DMR-0114154 and NSF DMR-0116567. Data for this study were measured at beamline X21 of the National Synchrotron Light Source (NSLS). Financial support comes principally from the Offices of Biological and Environmental Research and of Basic Energy Sciences of the U.S. Department of Energy.

[1]E. J. Tarsa, B. Heying, X. H. Wu, P. Fini, S. Den Baars, and J. S. Speck, J. Appl. Phys. **82**, 5472 (1997).
[2]B. Heying, R. Averbeck, L. F. Chen, E. Haus, H. Riechert, and J. S. Speck, J. Appl. Phys. **88**, 1855 (2000).
[3]B. Heying, I. Smorchkova, C. Poblenz, C. Elsass, P. Fini, S. Den Baars, U. Mishra, and J. S. Speck, Appl. Phys. Lett. **77**, 2885 (2000).
[4]J. E. Northrup and J. Neugebauer, Phys. Rev. B **60**, 8473 (1999).
[5]L. X. Zheng, M. H. Xie, and S. Y. Tong, Phys. Rev. B **61**, 4890 (2000).
[6]G. Koblmuller, R. Averbeck, H. Riechert, and P. Pongratz, Phys. Rev. B **69**, 035325 (2004).
[7]C. Adelmann, J. Brault, D. Jalabert, P. Gentile, H. Mariette, G. Mula, and B. Daudin, J. Appl. Phys. **91**, 9638 (2002).
[8]M. McLaurin, B. Haskell, S. Nakamura, and J. S. Speck, J. Appl. Phys. **96**, 327 (2004).
[9]S. Guha, N. A. Bojarczuk, and D. W. Kisker, Appl. Phys. Lett. **69**, 2879 (1996).
[10]G. Renaud *et al.*, Science **300**, 1416 (2003).
[11]A. S. Özcan *et al.* (unpublished).
[12]The Veeco website, http://www.veeco. com, posts the vapor pressure data for different elements, including Ga.
[13]C. B. Alcock, V. P. Itkin, and M. K. Horrigan, Can. Metall. Q. **23**, 309 (1984).
[14]Peter Hammer, Miriam S. Tokumoto, Celso V. Santilli, Sandra H. Pulcinelli, Aldo F. Craievich and A. Smith, J. Appl. Crystallogr. **36**, 435 (2003).
[15]J. Stangl, V. Holy, P. Mikulik, G. Bauer, I. Kegel, T. H. Metzger, O. G. Schmidt, C. Lange, and K. Eberl, Appl. Phys. Lett. **74**, 3785 (1999).
[16]A. S. Özcan *et al.* (unpublished).
[17]P. Guenard, G. Renaud, A. Barbier, and M. GautierSoyer, Surf. Rev. Lett. **5**, 321 (1998).
[18]R. P. Burns, K. A. Gabriel, and D. E. Pierce, J. Am. Ceram. Soc. **76**, 273 (1993).
[19]T. Mano, K. Watanabe, S. Tsukamoto, H. Fujioka, M. Oshima, and N. Koguchi, J. Cryst. Growth **209**, 504 (2000).
[20]J.-M. Lee, D. H. Kim, H. Hong, J.-C. Woo, and S.-J. Park, J. Cryst. Growth **212**, 67 (2000).
[21]J. A. Blackman and S. Brochard, Phys. Rev. Lett. **84**, 4409 (2000).
[22]S. Ulrich, S. Stoll, and E. Pefferkorn, Langmuir **20**, 1763 (2004).
[23]F. Family and P. Meakin, Phys. Rev. A **40**, 3836 (1989).